Radical scavenging property of a novel peptide derived from C-terminal SOD domain of superoxide dismutase enzyme in *Arthrospira platensis*

Anbazahan Sannasimuthu[a], Venkatesh Kumaresan[a], Mukesh Pasupuleti[b], Bilal Ahmad Paray[c], Mohammad K. Al-Sadoon[c], Jesu Arockiaraj[d],*

[a] *Department of Biotechnology, Faculty of Science and Humanities, SRM Institute of Science and Technology, Kattankulathur, 603 203 Chennai, Tamil Nadu, India*
[b] *Lab PCN 206, Microbiology Division, CSIR-Central Drug Research Institute, B.S. 10/1, Sector 10, Jankipuram Extension, Sitapur Road, Lucknow 226 031, Uttar Pradesh, India*
[c] *Department of Zoology, College of Science, King Saud University, PO Box 2455, Riyadh 11451, Saudi Arabia*
[d] *SRM Research Institute, SRM Institute of Science and Technology, Kattankulathur, 603 203 Chennai, Tamil Nadu, India*

ARTICLE INFO

ABSTRACT

Superoxide dismutase (SOD) is an evolutionary conserved detoxification enzyme and powerful antioxidant which defends against the elevated ROS that are induced by various stresses. *Arthrospira platensis* (*Ap*) is known for its antioxidant-mediated immunostimulant properties, but there is no report on the SOD dependent anti-oxidant mechanism. Therefore, in this study, we have analysed the effect of H_2O_2 on growth and pigment composition in spirulina. Results showed that spirulina exposed to 10 mM H_2O_2 showed elevated growth pattern as well as increase in chlorophyll pigment composition especially during early days of exposure. Gene expression results showed that the expression profile of *Ap*SOD during oxidative stress stimulated by 10 mM H_2O_2 at different time intervals (0, 5, 10, 15 and 20 days) with highest expression on day 10 post-exposure. Together, the results confirmed the antioxidant role of *Ap*SOD in spirulina during oxidative stress induced by H_2O_2. Based on the amino acid arrangement and composition, we have predicted a short peptide [160]LGLDVWEHAYYL[171] (LL12) from the catalytic centre of C-terminal SOD domain; further the peptide was synthesized. Antioxidant assays showed that LL12 peptide critically involved in radical scavenging mechanism. Also, LL12 peptide reduced the intracellular ROS level in H_2O_2 exposed leucocytes at a concentration of 12.5 μM. Cytotoxicity assay was performed on human leucocytes which showed that LL12 did not exhibit any cytotoxic activity against any of the leucocytes population. Overall, the study highlights the radical scavenging property of a novel short peptide derived from the C-terminal domain of *Ap*SOD which have the potential to develop as a biopharmaceutical drug.

1. Introduction

During energy production and other metabolic process in living organisms, reactive oxygen species (ROS) such as hydrogen peroxide (H_2O_2), superoxide radical (O_2^-) and hydroxyl radical (^-OH) are generated as by-products due to oxygen metabolism. ROS, especially H_2O_2, disrupts the physiological balance in tissues by degrading the cellular components such as lipids, proteins and nucleic acids [1]. H_2O_2 is generated as by-products of various metabolic processes such as photosynthesis and respiration in microalgae and plants [2] which are mainly involved in key signalling pathways in development and stress responses. In freshwater and marine environments, H_2O_2 is commonly found at high concentrations such as 10 *pM* and it varies between 0.5 and 200 nM in sea water and up to 800 nM in freshwater lakes [3]. In freshwater ecosystem, high concentration of H_2O_2 can either harm or damage the cells of aquatic animals or prompt acclimation at moderate levels. H_2O_2 also acts as an intracellular precursor for more reactive oxidants as it moves rapidly across the membranes by diffusion [4]. Although, higher concentration of H_2O_2 is toxic to many aquatic organisms such as fish and shellfish; microalgae such as spirulina can withstand and grow as they exhibit unique antioxidant mechanisms to sustain and detoxify the elevated free-radicals and thus protect their cellular parts from uncontrolled oxidative damages [5]. The primary ROS scavenging enzymatic defense mechanism encompasses super-oxide dismutase (SOD), glutathione peroxidase, (GPX), catalase (CAT) and peroxiredoxin (PrxR) [6].

SOD is one of the crucial antioxidant enzymes which primarily involves in the conversion of superoxide radicals (O_2^-) into O_2 and H_2O_2,

---

* Corresponding author.
E-mail address: jesuarockiaraj.a@ktr.srmuniv.ac.in (J. Arockiaraj).

thus protecting the cells and tissues from oxidative damage [7]. SODs are highly conserved metallo-enzymes which are categorised into four evolutionarily divergent groups based on their metal cofactor such as iron SOD (FeSOD), manganese SOD (MnSOD), nickel SOD (NiSOD), and copper/zinc SOD (Cu/Zn SOD). FeSODs are predominantly found in many bacteria, microalgae and plants [49]; NiSODs are found in microscopic organisms particularly in *Streptomyces* sp. [8] and MnSODs and Cu/ZnSODs are found in wide range of organisms especially in aquatic organisms [9,10]. SOD in microalgae plays a key role in protecting the cells from oxidative stress induced by various methods including chemical and biological stresses, heavy metals and radiations. Among all SODs, FeSOD is commonly found in majority of the microalgae and diatoms. Ismaiel et al. [11] reported that iron containing SOD may play a role in the survival of spirulina under stress conditions. FeSOD potentially responds to the H_2O_2 stress and protects cyanobacteria cells against O_2^- formed within the cytosol along with MnSOD which protects against O_2^- formed in the thylakoid lumen.

Arthrospira platensis (*A. platensis*) is mainly considered as a suitable immune-stimulant and natural antioxidant to humans and animals [12]. Spirulina is one of the well-studied microalgae with an extensive nutritive and therapeutic properties such as anti-cancer [13], anti-virus [14], anti-inflammatory [15,16], immune-stimulant [17], fatty-liver-preventing [18], neuroprotective [19] and cardio protectant [20]. Abd El-Baky et al. [4] reported that the antioxidant mechanism of *A. platensis* protected the cells up to 8 mM H_2O_2. So far, few antioxidant peptides with notable radical scavenging properties have been purified and derived from various sources such as plants, invertebrates, birds and higher vertebrates [21–24]. Recently, Jie et al. [25] reported that the hydrolysate of *A. platensis* comprises of unique antioxidant peptides, which might act as good source for therapeutics. Generally, the antioxidant activity of such short peptides is strongly influenced by their molecular mass, amino acid compositions, arrangement, structure and hydrophobicities [26]. These peptides involve in antioxidant reactions by acting as inhibitors of lipid peroxidation, chelators of transition metal ions or scavengers of free radicals by donating hydrogen. Thus, peptides acting as hydrogen donors serve as an excellent antioxidant peptide involving in multiple free radical scavenging mechanisms.

In this study, a superoxide dismutase (*Ap*SOD) sequence was identified from the cDNA library of *A. platensis* developed by Illumina NextSeq500 technology. The identified full length cDNA sequence was reconfirmed by sequencing and BLAST alignment. Further, the physicochemical parameters of the cDNA sequence and its derived protein sequence were analysed. The effect of different concentrations of H_2O_2 on the growth of spirulina cells was evaluated and the modulation of *Ap*SOD transcripts during H_2O_2 stress in spirulina live culture was analysed using qRT-PCR analysis. To understand the antioxidant efficacy of the SOD domain region, a short peptide (LL12) was identified from the C-terminal region of Fe/Mn SOD based on the molecular mass, amino acid compositions, structure, sequences, hydrophobicities and evolutionary conserved region. The peptide (LL12) was synthesized chemically and its antioxidant mechanism was determined by various activity assays. In addition, the non-toxic nature of the peptide was confirmed by exposing human blood leucocytes to the peptides. Moreover, determination of intracellular ROS level was performed to confirm the radical scavenging activity of LL12 peptide to human blood leucocytes by flow cytometry.

2. Materials and methods

2.1. Spirulina cultivation

Water sample collected from Potheri Lake, Chennai (12.825527°N 80.039606°E) was microscopically examined for specific spirulina filaments with clear spiral morphology and diluted in sterile 6-well plates containing Zarrouk's medium until there is only one filament in the well. Further, the single cell was cultivated in modified Zarrouk's

medium under 12:12 (day/night) illumination conditions in a specialized culture hood [27]. We obtained permission from National Biodiversity Authority of India for carrying out research experiments using the isolated spirulina cells (NBA/Tech Appl/9/742/14/16–17/450). The cyanobacteria isolate was identified as *A. platensis* by 16S rRNA sequencing and the sequence was submitted to NCBI database (Accession No. KY393096) [28].

2.2. H_2O_2 stress, algal cells collection and pigment analysis

The isolated spirulina cells were acclimatized for 30 days prior to experimentation. For each challenge, a set of 3 culture flasks were tested along with control. H_2O_2 (30% w/w in H_2O, Sigma-Aldrich) stress was given to algal culture at 10 mM concentration. Control flasks were maintained without H_2O_2 stress. Then algal cells were collected from challenged and control spirulina culture flasks at 5 various time points including days 0, 5, 10, 15 and 20 of post-challenge. To understand the post-exposure symptoms of different concentrations of H_2O_2 in spirulina cells, we have carried out the experiment for up to 20 days. Spirulina cells were collected from each Erlenmeyer flask from culture grown at different concentrations of H_2O_2 at different time points. The kinetics study of *A. platensis* growth was carried out in order to examine the ability of cellular growth of microalgae in every alternate day by measuring the optical density at 560 nm. Photosynthetic pigment chlorophyll a (Chl a), were quantified in *A. platensis* at different time points during H_2O_2 stress. Briefly, 0.5 g of the cells was grinded using 5 ml of 100% acetone (Fisher Scientific) for complete extraction of the pigments. Further, extracted pigments were centrifuged at 500 × g for 5 min and the supernatant was collected and the concentrations were determined using UV spectrophotometer (Shimadzu, Japan). Following formula was used to calculate the pigment concentrations [29]: Chl a = 11.24 $A_{661.6}$–2.04 $A_{644.8}$ (μg/ml). All the spirulina cells were flash frozen in liquid nitrogen and stored at −80 °C until further use.

2.3. RNA isolation, cDNA synthesis and gene expression analysis

The spirulina cells were collected from the culture medium, filtered through a glass microfiber filter-GF/C (Whatman, Kent, UK) and total RNA was isolated using TRIzol solution (Life Technologies, Rockville, MD, U.S.A.) as per manufacturer's protocol. The quantity and purity of the isolated RNA was analysed using NanoDrop (Thermo Scientific, USA). Finally, the purified RNA was converted to cDNA using Transcriptor First Strand cDNA Synthesis Kit (Roche Diagnostics GmbH, Germany) according to the manufacturer's method with oligo (dT) as primer. The concentration of cDNA is unified as 100 ng in all the samples prior to analysis. qRT-PCR analysis was performed to quantify the transcripts of *Ap*SOD in normal cells and H_2O_2 treated cells, using Fast SYBR® Green Master Mix (Roche Diagnostics GmbH, Germany) in Light Cycler 96 Real Time PCR system (Roche). Relative quantification of *Ap*SOD gene was performed using 16S rRNA as internal control gene and the change in the folds of expression between control and treated cells were recorded. The primers designed previously by Kumaresan et al. [28] were used to amplify *Ap*SOD mRNA: *Ap*SOD F1, GGC TAA TAT GTC CCT GGA AGA G (Sense) and *Ap*SOD R2, AGA CTT GGG CAG CGT TAT T (Anti sense) and 16S rRNA (GenBank Accession No. KY393096): 16S rRNAF3, CGTAAA CCT CTC CTCAGT TCA G (Sense) and 16S rRNA R4, GAACGGATT CAC CGC AGT AT (Anti sense). Quantitative real time PCR assay was performed using the following cycles: 95 °C for 30 s, 40 cycles of 95 °C for 5 s and 58 °C for 60 s by means of a 20 μl qRT-PCR reaction mixture containing 2 μl cDNA, 10 μl Fast SYBR® Green Master Mix, 0.5 μl of each PCR forward/reverse primers and 7 μl nuclease-free water. To verify the purity of the amplification product, melting curve analysis was performed. Finally, the gene expression results were analysed by $2^{-\Delta\Delta CT}$ method using the Light Cycler 96 software (Version1.1.0.1320). The Cq values were recorded for each reaction and all the reactions were performed in

triplicates. The primer efficiency of the qRT-PCR primers have been calculated as 99.07% for 16S rRNA and 99.35% *Ap*SOD.

2.4. Identification of A. platensis SOD from transcriptome dataset

A full length cDNA sequence encoding *ApSOD* protein was identified from the transcriptome dataset of *A. platensis* established by Illumina NextSeq500 technology and the detailed methodology of transcriptome construction was provided in our earlier manuscript [27]. The identified cDNA sequence was validated using internal sequencing and the sequence was submitted to EMBL database (Accession No. LT667405). Translate tool from Expasy (https://web.expasy.org/translate/) was used to derive the protein sequence from the identified cDNA sequence and further sequence analysis were made using the derived putative sequence. Further, various gene parameters such as ORF, 5′ and 3′ untranslated regions, start and stop codons of the full length *Ap*SOD cDNA sequence were determined.

2.5. Sequence analysis of ApSOD

BLAST (http://blast.ncbi.nlm.nih.gov/Blast.cgi) analysis was performed to align the putative protein sequence with the other known protein sequences stored in NCBI database to screen the homologous sequences that are similar to *Ap*SOD protein sequence. Prot-Param tool on ExPASy (http://web.expasy.org/protparam/) was used to calculate various other parameters of the translated protein sequence such as theoretical isoelectric point (pI), molecular mass and instability index. The conserved domains present in the *Ap*SOD protein sequence was identified using NCBI Conserved Domain database (http://www.ncbi.nlm.nih.gov/Structure/cdd/wrpsb.cgi) based on the sequence homology. PROSITE database was used to determine the conserved motifs and profiles in *Ap*SOD (http://prosite.expasy.org/scanprosite/). SignalP tool was used to determine the putative cleavage site of the signal peptide (http://www.cbs.dtu.dk/services/SignalP/). To identify whether there are any transmembrane segments present in the *Ap*SOD protein, SACS MEMSAT2 tool (http://www.sacs.ucsf.edu/cgi-bin/memsat.py) was used. MultiLoc tool (http://abi.inf.uni-tuebingen.de/Services/MultiLoc/) was used to predict the subcellular location of *Ap*SOD. Multiple sequence alignment (MSA) analysis was performed to determine the conserved residues of *Ap*SOD with other homologous sequence using BioEdit (Version 7.0.0). To understand the structural features of *Ap*SOD, the protein sequence was submitted to I-TASSER program (http://zhanglab.ccmb.med.umich.edu/I-TASSER) and different structural models were predicted and the structural conformations were validated by Ramachandran plot analysis (http://mordred.bioc.cam.ac.uk/~rapper/rampage.php). The secondary structure of *Ap*SOD protein was evaluated using Polyview (http://polyview.cchmc.org) and the tertiary structure was viewed and analysed using PyMol tool (Version 0.99).

2.6. Antioxidant peptide identification and synthesis

Based on the following properties, a short peptide with putative antioxidant activity was determined: 1) arrangement of amino acids with potential antioxidant properties, 2) evolutionary conserved region among other cyanobacteria, 3) sequence located in the SOD domain region, 4) hydrophobicity and 5) molecular weight. After multiple-factor screening, a short peptide (LL12: LGLDVWEHAYYL) was identified from the C-terminal region of *Ap*Fe/MnSOD. The hydrophobicity and hydrophilicity property of LL12 peptide was confirmed by PEPTIDE 2.0 online tool (https://www.peptide2.com/peptide_synthesis_hydrophobicity_hydrophilicity.php). The structural conformation of LL12 peptide was predicted using PepDraw: an online Peptide Calculator and Predictor tool (http://www.tulane.edu/~biochem/WW/PepDraw/index.html).

The LL12 peptide was chemically synthesized (Zhengzhou Peptides

Pharmaceutical Technology Co., Ltd., China) and the integrity of the LL12 synthesized peptide has been verified as > 95% using HPLC coupled with MS (provided by the manufacturer). The synthesized peptide was dissolved in endotoxin free water and maintained as stock (1 mM) and stored at −20 °C until further use.

2.7. Determination of antioxidant mechanism by peptide

To understand the antioxidant mechanism exhibited by the peptide, the following antioxidant assays involving different analytical methods were performed:

2.7.1. Superoxide anion radical scavenging activity

The superoxide anion radical scavenging activity of the peptide was analysed using the method suggested by Chi et al. [30]. In the experiment, superoxide anion radical was generated in 50 μl of nitrotetrazolium blue chloride (2.52 mM), 50 μl of NADH (624 mM), and 50 μl of various concentrations of peptide (6.25 μM to 100 μM). The reaction was started by adding 50 μl of phenazine methosulfate solution (120 μg/ml) to the reaction mixture. The absorbance of the solution was measured at 560 nm (UV1800, SHIMADZU, Kyoto, Japan) against the control with blank after 5 min incubation at 25 °C. The ability of scavenging superoxide anion radical has been calculated using the following formula:

Superoxide anion radical scavenging activity (%)

$$= [(A_{control} − A_{sample})/A_{control}] \times 100\%$$

2.7.2. DPPH radical scavenging activity assay

The DPPH scavenging activities of the peptide become measured by a colorimetric method [31] with slight changes. An aliquot of 100 μl of test sample solution at various concentrations (6.25 μM to 100 μM) was mixed with 100 μl of readily prepared DPPH solution (0.1 mM) dissolved in 95% ethanol. Further, the reaction mixture was incubated in the dark for 30 min at room temperature. Finally, the absorbance of the reaction mixture was evaluated at 517 nm using a UV–Vis spectrophotometer (UV1800, SHIMADZU, Kyoto, Japan). Ethanol was used as negative control. All the experiments were performed in triplicates. The radical scavenging efficacy of the peptide was determined using the following formula.

$$DPPH \ radical \ scavenging \ activity \ (\%) = [(A_{control} − A_{sample})/A_{control}]$$
$$\times 100\%$$

2.7.3. Trolox equivalent antioxidant capacity (TEAC) (or) ABTS assay

TEAC assay was performed following to the method of Re et al. [32] with slight modifications. Briefly, 7 mM ABTS stock solution was mixed with 2.45 mM potassium persulfate to produce ABTS radical cation (ABTS$^{\cdot+}$). The mixture was then maintained at room temperature in the dark for 12 to 16 h earlier than use. Further, the reaction mixture was diluted to an absorbance of 0.70 ± 0.02 at 734 nm using 0.2 M PBS (pH 7.4) at 30 °C. Twenty microliter of the sample or Trolox at various concentrations (6.25 μM to 100 μM) was added to 180 μl of diluted ABTS$^{\cdot-}$ solution and incubated at 30 °C for 6 min. The decrease in absorbance at 734 nm was monitored using a spectrophotometer (UV1800, SHIMADZU, Kyoto, Japan) which is equivalent to the scavenging of radicals by the peptides. All the experiments were conducted in triplicates. The concentration of the peptide (at milliMolar) giving the similar decrease of ABTS$^{\cdot+}$ cation as that of 1 mM of trolox was considered as 'Trolox equivalent antioxidant capacity'.

2.7.4. Hydroxyl radical scavenging activity

The hydroxyl radical scavenging activity assay was performed following to the method described by Li et al. [33], with slight modification. A mixture of 30 μl of 1,10-phenanthroline (5.0 mM), 30 μl of

ethylenediaminetetraacetic acid (EDTA) (15 mM) and 30 μl of FeSO₄ (5.0 mM) was mixed with 30 μl of sodium phosphate buffer (0.2 M, pH 7.4). Further, 40 μl of peptides or trolox at different concentrations (6.25 μM to 100 μM) and 40 μl of H_2O_2 (0.03%) were added. The mixture of sample was incubated at 37 °C for 60 min, and the absorbance of the solution was measured at 536 nm (UV1800, SHIMADZU, Kyoto, Japan). All the experiments were conducted in triplicates. The antioxidant activity was calculated accordance with the trolox calibration curve and converted to the TEAC value.

2.8. Cytotoxic activity of LL12 on human leucocytes

To assess the toxicity of the LL12 peptide in normal cells, cytotoxicity analysis was conducted against blood leukocytes from human (Ethical Clearance No. CDRI/IEC/2014/A1). Human blood leucocytes (1×10^7 cells) were separated from whole blood using gradient centrifugation ($1500 \times g$ for 15 min at 4 °C) with Easy Sep™ RBC lysis buffer (STEMCELL™ Technologies). The cytotoxic effect of LL12 at a concentration of 100 μM on monocytes, granulocytes and lymphocytes population of human blood was determined by Cytomics FC 500 (BECKMAN COULTER Life Sciences, Indiana, USA). Triton X-100 and 1× PBS were used as positive and negative controls, respectively. All the reactions were performed in triplicates and the results were represented as mean ± standard deviation.

2.9. Determination of intracellular ROS level in leucocytes

Intracellular ROS generation was quantitatively determined by the method of Wan et al. [34] using the cell permeant probe 2′,7′-dichlorofluoresceindiacetate (DCFDA) dye by measuring the quantity of fluorescent dichlorofluorescein (DCF) formed within the human blood leucocytes using Cytomics FC 500 (BECKMAN COULTER Life Sciences, Indiana, USA). The amount of DCF formed will be directly proportional to the quantity of ROS present inside the cells. Briefly, cells seeded in black 96-well plate at a density of 10,000 cells/well were incubated with 10 μM DCFDA and 20 μl of 30% H_2O_2 was added into each well according to the concentrations that were decided to be used for 30 min at 37 °C followed by incubation with desired treatments of LL12 (6.25, 12.5, 25, 50, 100, 200 μM). After 2 h, intracellular ROS level was measured by flow cytometry while the cells were gated on FSC/SSC to remove debris and mean fluorescence intensity from 10,000 cells was acquired. Simultaneously, the reduction in ROS level on peptide treated blood leucocytes was analysed and the images were captured using confocal fluorescence microscope (ZEISS™, Jena, Germany) under 20× objective.

2.10. Statistical analysis

All the data given in the study is a mean of three duplicates ± standard deviation. For all the activity assay and gene expression study, we have performed a one-way ANOVA followed by Tukey's Multiple Range Test using SPSS 11.5 at 5% level.

3. Results and discussion

3.1. H_2O_2 stress on A. platensis cell growth

To understand the tolerance of external H_2O_2 stress by *A. platensis*, the culture media with spirulina cells treated with various concentrations of H_2O_2 (5, 10, 25, 50 and 100 mM) and its effect was monitored for a period of 24 days by measurement of OD value at 560 nm [4]. Results revealed that the growth of *A. platensis* cells was significantly ($P < 0.05$) affected by H_2O_2 (5 and 10 mM) stress in concentration dependent manner during the initial growth phase between day 0 and 6 (Fig. 1A). Further, there is an increase in the growth of *A. platensis i.e.*, 2, 5, 11, 15 days (17% of increase in OD value) compared to the control

on days 8, 12, 16, 20 and 24, respectively. Moreover, microscopic observation indicated that no bleaching of spirulina cells grown at low and high levels of H_2O_2 (10 and 100 mM) has been observed. As a result, the photosynthetic activity of *A. platensis* was not influenced by H_2O_2 stress up to 10 mM (Fig. 1B). However, higher concentrations (25, 50, 100 mM) of H_2O_2 significantly ($P < 0.05$) affected the growth of *A. platensis*. This showed the environmentally relevant concentration of H_2O_2 (< 10 mM), where spirulina was able to grow better than the control group [4].

3.2. Effect of H_2O_2 on chlorophyll of A. platensis

To correlate the effect of H_2O_2 (10 mM) on the growth pattern of *A. platensis* with that of the photosynthesis process, changes in different pigments concentration were determined spectrophotometrically at different time intervals (0, 5, 10, 15 and 20 days). Our results showed that Chl a content in spirulina was significantly ($P < 0.05$) increased with the time of exposure of H_2O_2 during initial growth phase than the control cells (Table 1). A similar condition of pigment modulation was observed in chlorella during oxidative stress induced by nitrogen starvation [35].

When the growth pattern of H_2O_2 exposed cells are compared with the Chl a pattern, it is inversely correlated with each other (*i.e.*) growth was affected during the initial phase of H_2O_2 exposure whereas Chl a concentration increased. This pattern indicates the role of chlorophyll pigments during oxidative stress. Also, increased Chl a content might have supported the growth of the cells which is evident by the growth pattern where the growth of H_2O_2 exposed cells was higher than the control cells during the mid-phase of growth (10–15 days). However, high concentration of H_2O_2 (100 mM) was significantly ($P < 0.05$) affected both pigment concentration and growth which clearly indicated that spirulina was able to survive up to 10 mM concentration of H_2O_2 that is far higher than the environmental concentration, thus signifying the effective antioxidant role of spirulina in aquatic ecosystems.

3.3. Gene expression analysis of ApSOD

To understand the H_2O_2 induced modulation of *Ap*SOD gene expression, the algal cells were challenged with 10 mM of H_2O_2 and compared with that of untreated at different time points post-treatment (p.t.) (0, 5, 10, 15 and 20 days). Results showed that H_2O_2 significantly ($P < 0.05$) increased the expression of *Ap*SOD gene on day 5, however the highest expression was found at day 10 ($P < 0.05$). Later, the expression level declined on day 15 and 20 which indicated that the expression level of SOD is getting back to the basal level of expression (Fig. 2) which confirms that the cells revived from stress without any post-exposure complications. This showed that *Ap*SOD plays a key role in maintaining the ROS level in the cells and prevent the cells from damage. Also the expression pattern correlates with the growth pattern and thus it is clear that the increased expression of *Ap*SOD was because of the action of H_2O_2 on the cells at the initial growth phase and due to the action of antioxidant role of *Ap*SOD, the cells were protected from damage and maintained the antioxidant homeostasis, thereby increasing the growth of the cells in an efficient manner. Therefore, we could conclude that *Ap*SOD plays a key role in antioxidant mechanism in spirulina and the unique feature of *Ap*SOD protein could reveal more potential antioxidant activity to combat against oxidative stress induced by H_2O_2. Our finding confirmed the antioxidant role of *Ap*SOD against H_2O_2 along with its other effects on the growth, pigment content, proline, malondialdehyde, photosynthetic activity and antioxidant enzyme activity in *A. platensis* [36]. Therefore, it is also possible to predict that *Ap*SOD gene expression can mitigate the effects and protect against a broad range of stresses.

A) Growth curve of *A. platensis*

Untreated cells　　　Cells + 10 mM H_2O_2　　　Cells + 100 mM H_2O_2
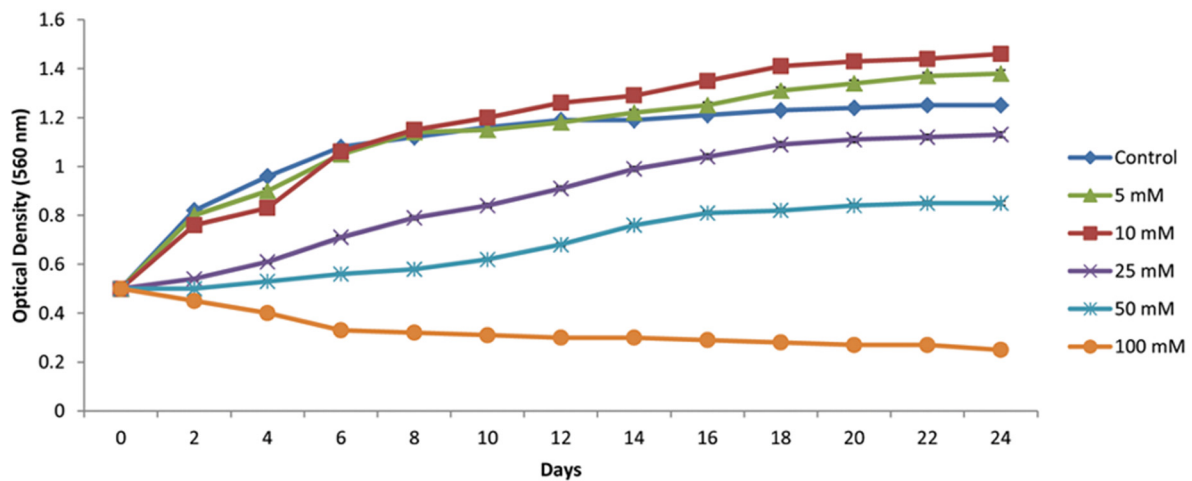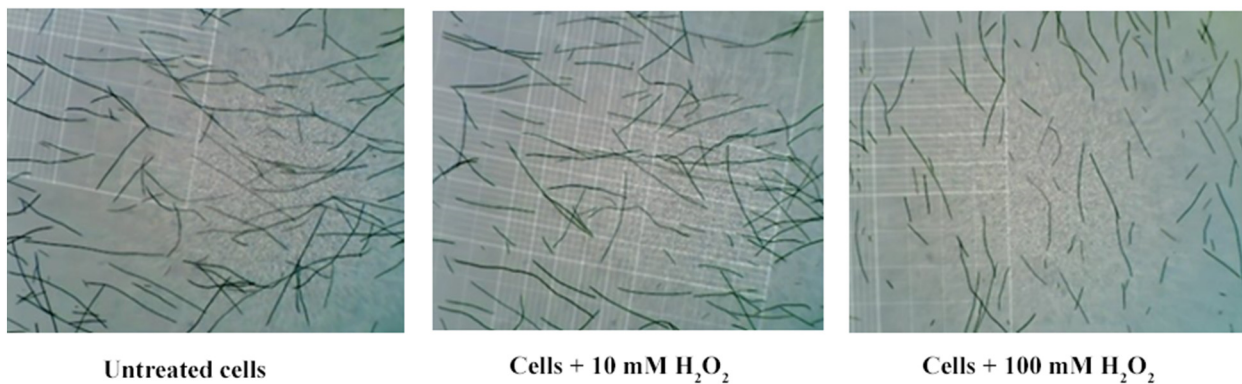
B) Microscopic view of *A. platensis* cells treated with H_2O_2

Fig. 1. Effect of H_2O_2 on *A. platensis* cells. A) Comparative growth curve of *A. platensis* cells treated with different concentrations of H_2O_2 (0, 5, 10, 25, 50 and 100 mM) for a period of 24 days where elevated growth was observed in 10 mM H_2O_2 between 8 and 24 days. Data shown is the mean $\pm$ SD, $n = 3$. B) Comparison of microscopic view of H_2O_2 (10 mM) treated *A. platensis* and untreated cells revealing no morphological changes between control and treated cells, however cell breakage was observed in cells treated with 100 mM H_2O_2.

Table 1

Modulation of chlorophyll pigment concentration during H_2O_2 stress in *A. platensis* at different time points (0, 5, 10, 15 and 20 days). Data shown is the mean $\pm$ SD, $n = 3$.

Day		Chl *a* (µg/ml)
0		2.837 ± 0.165
5	$-H_2O_2$	7.271 ± 0.214
	$+H_2O_2$	8.001 ± 0.302
10	$-H_2O_2$	12.678 ± 0.543
	$+H_2O_2$	14.816 ± 0.430
15	$-H_2O_2$	24.761 ± 0.506
	$+H_2O_2$	25.524 ± 0.327
20	$-H_2O_2$	31.583 ± 0.735
	$+H_2O_2$	32.090 ± 0.701

3.4. ApSOD sequence analysis

We have identified a full length cDNA sequence (606 nucleotides) from the transcriptome library of spirulina which encoded *Ap*SOD protein (201 residues) comprising of 13 positively charged and 21 negatively charged residues. The predicted molecular weight of the protein was 22,095 Da and theoretical isoelectric point (pI) of 5.11. The protein was considered as a stable protein with an instability index of 25.91. No signal sequence was predicted by signal peptide prediction
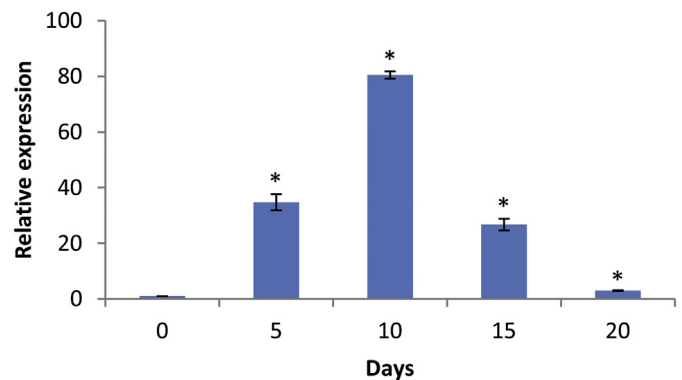

Fig. 2. H_2O_2 induced gene expression modulation in *A. platensis*. The modulated expression of superoxide dismutase (*Ap*SOD) post-H_2O_2 challenge in *A. platensis* quantified by qRT-PCR at different time points (0, 5, 10, 15 and 20 days). The highest expression of *Ap*SOD mRNA was observed at 10th day of post-treatment (p.t.) and the expression level declined to the basal level between 15th and 20th day p.t. Data shown is the mean $\pm$ SD, $n = 3$. The asterisk (*) denotes the significant different between control (day 0) and treatments (day 5, 10, 15 and 20) at $P < 0.05$ level by one-way ANOVA followed by Tukey's multiple range test.

```
Arthrospira platensis   MAFELPSLPFDQDALESSKMSANTLSYHHGKHHAAYVKNLNAAIEGTDMANMSLEEIIKATYNDPSKSGI 70
Planktothrix agardhii   MAFELPALPFADDALESSKMSAKTFSFHHGKHHAAYVTNLNKLIDGTGLADKSLEEIIKATANDPNKAGI 70
Limnoraphis robusta     MAFELPELPYAADALESSGMSKETFSYHHGKHHAAYVKNLNGMIEGTDLAGSSLEEIVKATANDPGKAGI 70
Lyngbya aestuarii       MAFELPELPYPADALESSGMSKQTFSFHHGKHHAAYVKKLNGMIEGTDLANKSLEEIVKATANDPSKSGI 70
Pleurocapsa minor       MAYELPALPYDYTALEP-VISKKTLEFHHDKHHAAYVNNYNSAVKGTEFENKSIEEVIKAVAGDSSKTAI 69

Arthrospira platensis   FNNAAQVWNHSFFWKCLKPNGGGQPTGALADKIQADFGSFDAFIQEFKNAAATQFGSGWAWLVLDNGTLK 140
Planktothrix agardhii   FNNAAQVWNHTFFWNSLKAGGGGQPTGALADKINADFGSFDKFIEEFKAAATTQFGSGWAWLVLNNGTLK 140
Limnoraphis robusta     FNNAAQVWNHSFFWHCMKPGGGGKPDGALAEKITADFGSYEAFVEEFKKAAATQFGSGWAWLVLDNGTLK 140
Lyngbya aestuarii       FNNAAQVWNHSFFWKCMKPGGGGKPSGALAEKINADFGSYEKFAEEFKNAGATQFGSGWAWLVLENGTLK 140
Pleurocapsa minor       FNNGAQAWNHTFYWNCMKPNGGGTPSGALADKIKADFGSFDKFVEEFKTAGATQFGSGWAWLVLDNGTLK 139

Arthrospira platensis   VTKTANAVNPMVEGKTPLLLGLDVWEHAYYL-FQNARPGFIDNFIENLVNWDFVAENLASAS 201
Planktothrix agardhii   VTKTANAGTPIVDGLTPLLT-LDVWEHAYYLDFQNARPAYIENFLNQLVNWDFVAENLAAA- 200
Limnoraphis robusta     VTKTANAANPIVEGAIPLLT-LDVWEHAYYLDFQNARPGYIENFLEKLVNWDFVAENLAAA- 200
Lyngbya aestuarii       VKKTLNAINPIIEGVTPLLT-MDVWEHAYYLDFQNARPGYIDNFLGKLVNWDFVAENLAAA- 200
Pleurocapsa minor       VTKTPNADNPIVAGQVPLLT-MDVWEHAYYLDYQNRRPDYINEFISKLINWDFVAQNFAAAS 200
```

A) Multiple sequence alignment of *Ap*SOD
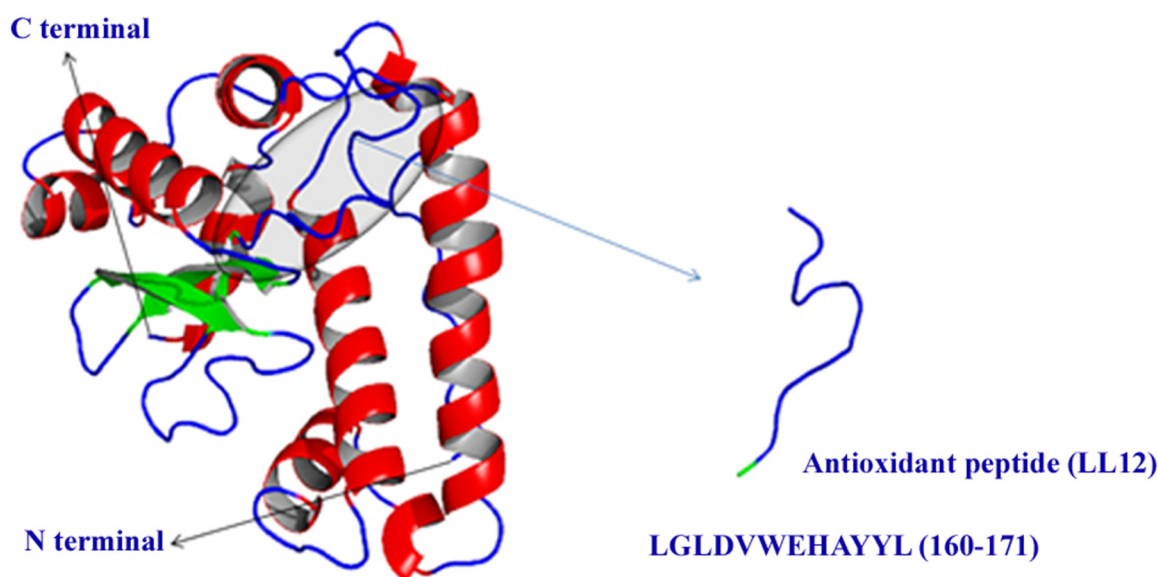
B) Three dimensional structure of *Ap*SOD

Fig. 3. Structural features of *Ap*SOD protein. A) Multiple sequence alignment of *Ap*SOD LL12 with other SOD species such as *Planktothrix agardhii*, *Limnoraphis robusta*, *Lyngbya aestuarii* and *Pleurocapsa minor*. The antioxidant peptide region is highlighted separately, highly conserved residues are marked in pink color and the similar residues are in Purple color. The residues which are highly varied are represented in light blue color. The conserved residues are represented in dark blue. B) Three dimensional structure of *Ap*SOD highlighting the antioxidant peptide region from the C-terminal domain. The red spirals denote the helix region and the blue lines represent the coil region. The antioxidant peptide residues are highlighted as blue colored coils with numbers representing the location (L_{160}–L_{171}). (For interpretation of the references to color in this figure legend, the reader is referred to the web version of this article.)

tool and cellular location analysis showed that the maximum probability (0.94) to be located in cytoplasm (Data not shown).

BLAST analysis exhibited that *Ap*SOD protein sequence showed maximum similarity with SOD of other algae specifically *Limnoraphis robusta* (80%), *Planktothrix agardhii* (78%) and *Lyngbya aestuarii* (78%). But *Ap*SOD sequence does not remain conserved with vertebrates and invertebrates. The percentage of similarity between *Ap*SOD and other related sequences are represented in Fig. 3A. This showed the unique nature of *Ap*SOD and it is possible to use its potential antioxidant property in higher organisms like human during oxidative stress caused by infection and chemical stress.

3.5. Structure analysis and peptide prediction

Conserved domain database (CDD) search resulted with two distinct SOD domains. The N-terminal SOD domain (pfam00081) is located between A^2 and K^{88} followed by C-terminal SOD domain (pfam02777) between P^{95} and N^{196} with a Fe/Mn binding site which belongs to iron/manganese binding superfamily. Multiple sequence alignment of *Ap*SOD with other known Fe/Mn sequences obtained from NCBI database revealed that there are many conserved residues between the selected sequences. This represents the significance of the SOD sequence which remained evolutionarily conserved between all the selected microalgae. Farvin et al. [37] reported the significance of the amino acids at the C-terminal of antioxidant proteins which play important roles in antioxidant mechanism than those at the N-terminal regions. Especially, bulky hydrophobic amino acids at the C-terminal were particularly involved in the antioxidant activity of those proteins. Suetsuna et al. [38] reported that the C-terminal sequence of SOD domain was necessary for the antioxidant function in oyster, *Crassostrea gigas*. Also, the electron donating ability of these proteins significantly influences the antioxidant activity in the free radical systems. Moreover, the

presence of three *N*-Myristoylation sites, one putative *N*-glycosylation site in the C-terminal domain is also suspected to influence the antioxidant activity of *Ap*SOD. Therefore, the C-terminal region of the *Ap*SOD protein plays a major role in the metal binding and subsequent radical scavenging process.

The structure of the *Ap*SOD sequence was predicted using I-TASSER (Iterative Threading ASSEmbly Refinement) based on the previously solved SOD protein structures which revealed that 51.24% of amino acids are located in α-helix region, 38.81% amino acids in coil region and 9.95% in ß-sheet region. Twelve distinct α-helices were found in the protein which is a conserved feature among Fe/Mn SOD where Fe/Mn binding sites were distributed in both coil and helix region (Fig. 3B). The Fe/Mn SOD signature sequence, [163]DVWEHAYY[170] which is the conserved metal binding domain was located in the coil region and remained conserved among the homologous SOD proteins. Although the metal binding function of the signature sequence was well characterized, the antioxidant roles of this sequence were not studied so far. Therefore, the conserved peptide sequence, [160]LGLDVWEHAYYL[171] (LL12) which contains the conserved catalytic residues D[163] and Y[170] was predicted with putative antioxidant activity and was synthesized chemically and its antioxidant activities were determined.

3.6. Characterization of antioxidant peptide

Structurally, the predicted peptide sequence LL12 was not found in either helix or sheet. Generally, it is a known fact that the antioxidant activity of the peptide was not because of any particular structural conformation, rather the arrangement of specific amino acids in a particular sequence [39]. Antioxidant peptide database prediction showed that the antioxidant peptide LL12 comprised of at least 7 residues with hydrophobic activity which might contribute to the antioxidant activity of the peptide. It has been reported that among the 20 essential amino acids, Trp, Tyr, Met, Cys, His and Phe exhibit potential antioxidant activity [40]. Cojocaru et al. [41] reported that Leu and Val reduces the serum levels of SOD and GPx which enlighten the role of Leucine-rich LL12 peptide in reactive oxygen scavenging.

3.7. Antioxidant mechanism of LL12

3.7.1. Superoxide anion radical scavenging activity of LL12

Lipid oxidation which is initiated by the perhydroxyl radicals in the form of releasing metalloprotein can promote oxidative reaction due to its ability in reducing transition metals. In living cells, superoxide dismutase (SOD) enzymes involve in the defense mechanism against the reactive oxygen for cytoprotection and it catalyse the neutralization of superoxide anion to hydrogen peroxide. During SRSA assay, superoxide anions which are generated in PMS/NADH-NBT systems by oxidation of PMS/NADH coupling reaction reduce NBT. The radical scavenging activity of LL12 for superoxide radicals was determined and the levels of superoxide anions reduced with increasing concentration of the peptide (Fig. 4A). LL12 could effectively ($P > 0.05$) scavenge the superoxide radicals (79.94 $\pm$ 1 at 6.25 μM) than the standard antioxidant trolox (67.92 $\pm$ 0.9 at 6.25 μM). The EC$_{50}$ value of the LL12 peptide has been determined as 12.3 μM. Suetsuna et al. [38] reported that casein protein contains YFYPEL peptide and it has a strong superoxide radical scavenging activity with an IC$_{50}$ value of 79.2 μM. Qian et al. [42] indicated that the oyster protein contains LKQELEDLLEKQE peptide and it has a potent superoxide radical scavenging activity with an IC$_{50}$ value of 78.97 μM. In living cells, short peptides scavenge the superoxide radicals due to that peptide could have a high SOD like activity. Overall, the highest superoxide radicals scavenging activity of LL12 suggested that the peptide derived from the C-terminal SOD domain of *Ap*SOD was far superior to the previously reported peptides.

3.7.2. DPPH radical scavenging activity

To evaluate the antioxidant activity of LL12 peptide, DPPH was used as a substrate. This assay is based on the reduction of DPPH in ethanol solution with a substance that can donate a hydrogen atom, due to the formation of the non-radical form DPPH-H by the reaction. LL12 was able to quench the stable radical DPPH and the decolorisation of DPPH was observed at higher concentration (Fig. 4B). Result showed that the radical scavenging activity of LL12 was not much significant at lower concentration (3.41 $\pm$ 0.55 at 6.25 μM) but higher concentration of LL12 displayed significant level ($P < 0.05$) of radical scavenging activity (52.89 $\pm$ 0.80 at 200 μM). However, the activity of LL12 was better than those of *A. platensis* hydrolysate 85.21 $\pm$ 1.59% at 10 mg/ml [25] and ethanol-soluble protein hydrolysate (PYFNK) of *Sphyrna lewini* (4.11 mg/ml) [43]. Thus, this research finding is in agreement with previous studies that suggested hydrolysates or peptides with lower MWs show higher free-radical scavenging activity [44].

3.7.3. Trolox equivalent antioxidant capacity (TEAC)

To evaluate the total antioxidant activity, ABTS radical cation decolorization assay was performed. This is one of the commonly used methods which is used to determine the activity of both lipophilic and hydrophilic samples [50]. In this study, the ABTS radicals inhibition percentage between LL12 and trolox was correlated (Fig. 4C). Results showed that the inhibition of ABTS radicals by LL12 was concentration dependent and highest inhibition concentration was determined as 97.28 $\pm$ 0.3 at 200 μM in comparison with the standard antioxidant trolox 95.86 $\pm$ 0.5 at 200 μM. This showed that the LL12 peptide exhibited ($P > 0.05$) a potential antioxidant potential equivalent to trolox.

3.7.4. Hydroxyl radical scavenging activity

Hydroxyl radicals are the most biologically active radicals, which can directly reacts with all the biological macromolecules such as DNA, RNA, and proteins and cause severe cellular damage [45]. Hence, to deactivate the hydroxyl radical, exogenous antioxidants would be necessary for balancing the redox state in the cells. In this experiment, hydroxyl radical was generated by the Fenton reaction (Fe2^{+} + H$_2$O$_2$) and the potential of LL12 peptide in scavenging hydroxyl radical was determined. The LL12 peptide showed potent antioxidant activity and the scavenging of hydroxyl free radical activities was higher (65.73 $\pm$ 0.43 at 6.25 μM) than the standard antioxidant trolox (59.86 $\pm$ 0.34 at 6.25 μM) and the highest ($P > 0.05$) inhibition concentration value of the synthetic peptide was 95.02 $\pm$ 0.49 at 200 μM in comparison with the standard antioxidant trolox value 94.59 $\pm$ 0.5 at 200 μM (Fig. 4D). Recently Guo et al. [46] reported that the hydroxyl radical scavenging activity of peptide which contain tyrosine rich (Lys-Tyr, Arg-Tyr, Tyr-Tyr) it exhibited ($P > 0.05$) potent antioxidant activity (76.2 $\pm$ 0.7, 74.6 $\pm$ 1.3 and 70.9 $\pm$ 0.9%) and hydrogen peroxide (43.5 $\pm$ 2.6, 44.7 $\pm$ 4.6 and 86.2 $\pm$ 0.8%). This suggested that the presence of tryptophan and tyrosine in LL12 may involve the hydroxyl radical scavenging activity.

Overall, the antioxidant potential of LL12 peptide was observed to be higher than the trolox standard which highlights the efficacy of the peptide as a potential antioxidant. Moreover, the cumulative results of all the above four assays indicated that the potential of the peptide was specifically because of the hydrogen donating capability of the amino acids in the specific sequence especially the presence of tryptophan and tyrosine at the C-terminal. However, further studies are required to confirm the above claim.

3.8. Cytotoxicity of LL12 on human leucocytes

Host cytotoxicity is one of the major limiting factors for using peptides as a therapeutic agent [47]. Therefore, the cytotoxicity of LL12 peptide was analysed against human blood leucocytes by analysing the change in population pattern of blood cells before and after exposure of peptide. Our results showed that, even at highest concentration of LL12
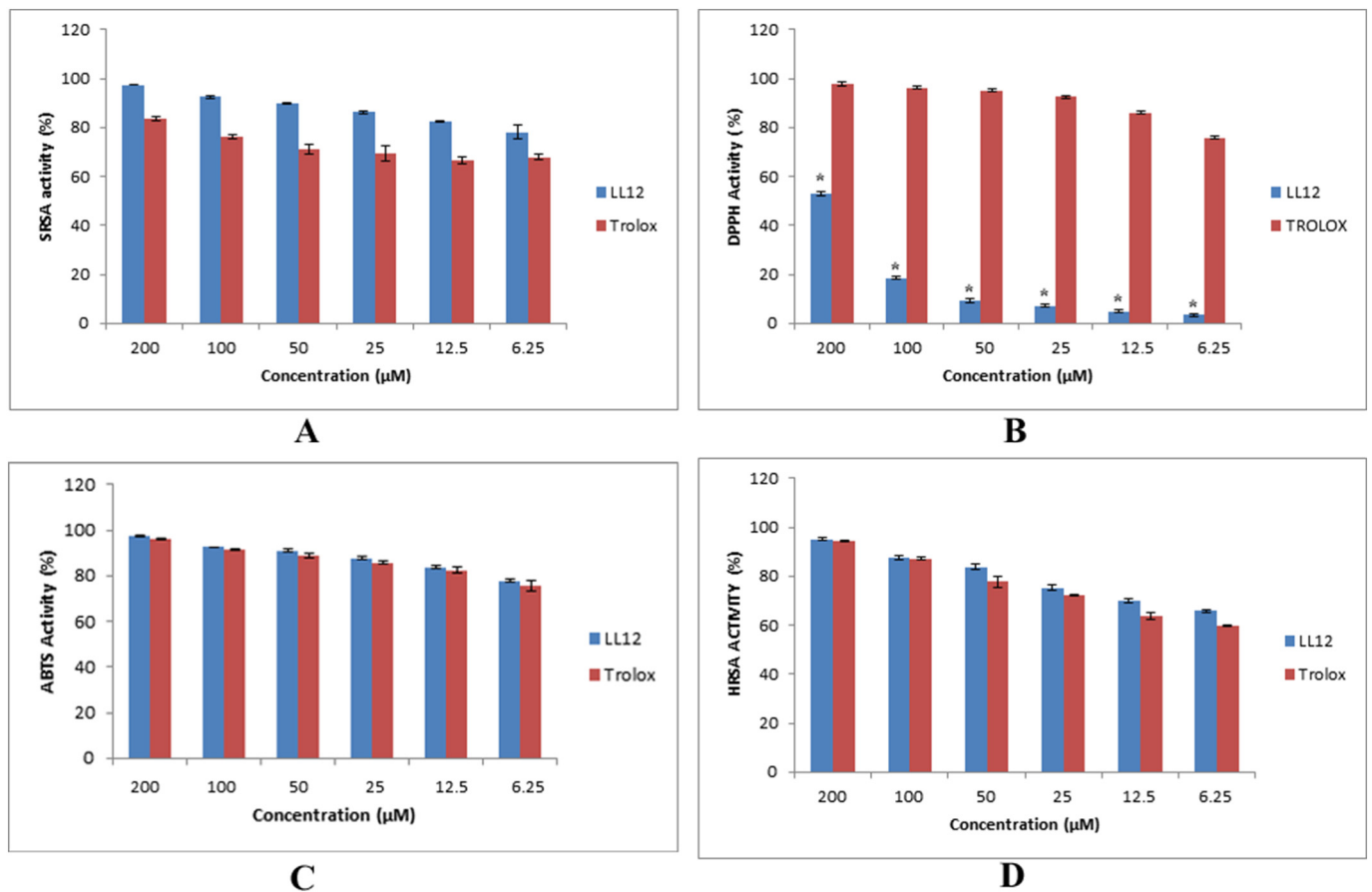
Fig. 4. Radical scavenging activity of the LL12 peptide. A) The superoxide radical scavenging ability of LL12 peptide was compared with that of standard antioxidant, Trolox by superoxide radical scavenging assay where LL12 exhibited superior radical scavenging activity than the standard. B) DPPH assay shows no significant hydrogen donating activity by LL12 peptide when compared with Trolox. The asterisk (*) denotes the significant different between control (Trolox) and treatments (200, 100, 50, 25, 12.5 and 6.25 μM) at $P < 0.05$ level by one-way ANOVA followed by Tukey's multiple range test. C) TEAC assay reveals the Trolox equivalent capacity of LL12 in scavenging the ABTS radicals. D) HRSA assay exhibits the scavenging activity of hydroxyl ions. Except DPPH assay, LL12 peptide showed significant radical scavenging activity in comparison with standard, Trolox. Data shown is the mean ± SD, $n = 3$.
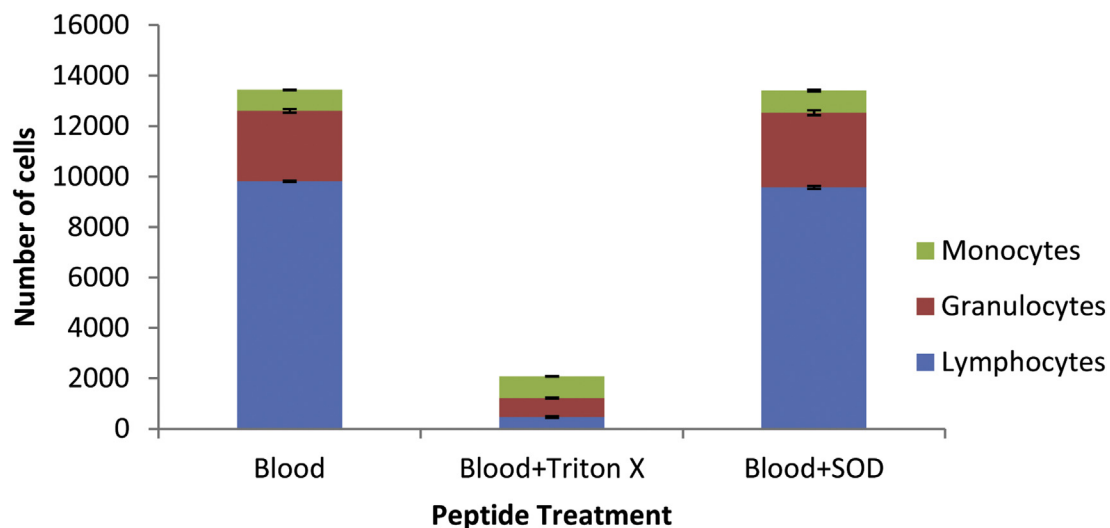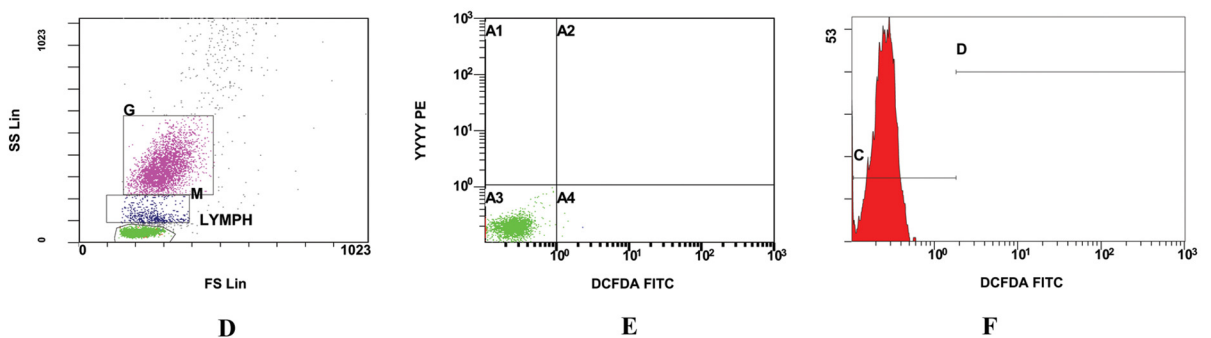

Fig. 5. Cytotoxicity of LL12 on human leucocytes. Cytotoxicity activity was determined against blood leucocytes in the presence or absence of highest concentrations of LL12 (100 μM). Phosphate buffered saline was used as negative controls and TritonX used as positive control. LL12 exhibited no significant cytotoxicity activity against human blood leucocytes. Data shown is the mean ± SD, $n = 3$.

(100 μM) treatment, no significant difference in blood cell population was observed with that of the untreated cells, whereas, Triton X 100 (positive control) significantly ($P < 0.05$) reduced the cell numbers of all the leucocytes population of human blood (Fig. 5). Thus, the results showed that LL12 neither exhibit cytotoxicity nor proliferative activity against human blood leucocytes in any of the experimented
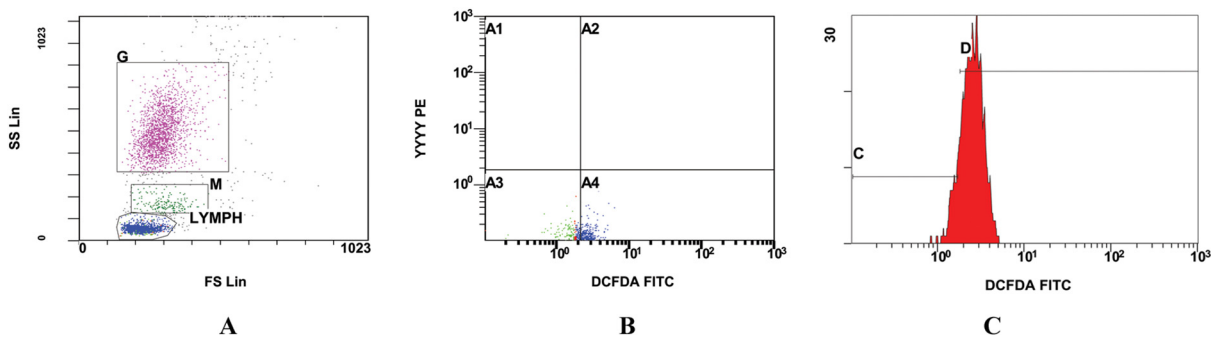
H₂O₂ induced increase of intracellular ROS level in human leucocytes

Reduction of intracellular ROS in human leucocytes by LL12

G) Blood+DCFDA+H₂O₂ (DF)   H) Blood+DCFDA+H₂O₂ (BF)

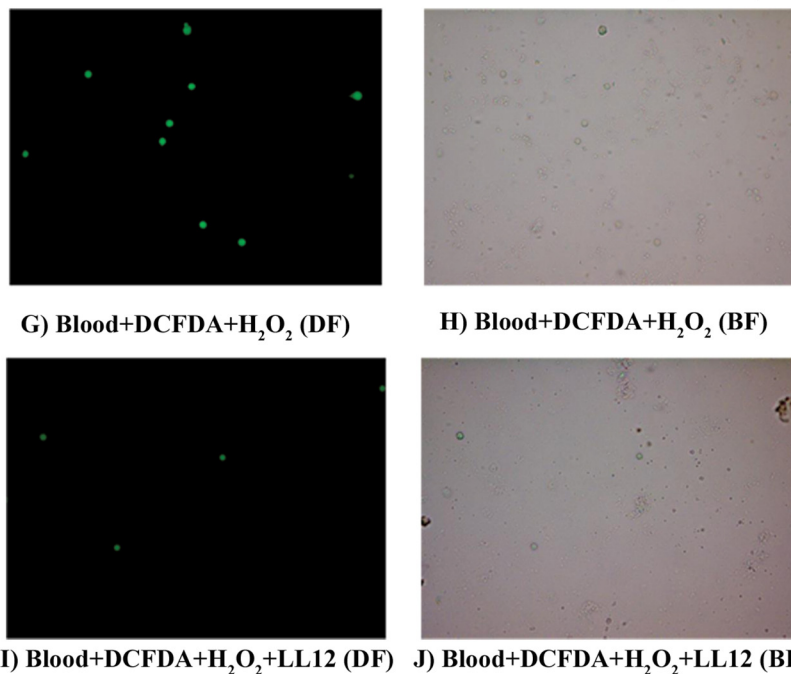I) Blood+DCFDA+H₂O₂+LL12 (DF)   J) Blood+DCFDA+H₂O₂+LL12 (BF)

Fig. 6. Intracellular Reactive Oxygen Species (ROS) scavenging ability of LL12 peptide on human leucocytes. Intracellular ROS level in leucocytes were determined by fluorescence dye DCFDA using FACS: A) Blood profile after treatment with 2 mM H_2O_2; B) Fluorescence shift in DCFDA due to high ROS level; C) Histogram showing the shift in fluorescence indicating the increased ROS level in H_2O_2 treated leucocytes; D) Blood profile after treatment with LL12 peptide and 2 mM H_2O_2; E) No fluorescence shift due to ROS scavenging activity of LL12 peptide; F) Histogram showing no shift in fluorescence peak due to minimum level of ROS in leucocytes. Data shown is the mean $\pm$ SD, $n = 3$. Fluorescence imaging showed the real time ROS level captured by confocal microscopy: G) Dark field image showing fluorescence exhibited by ROS-DCFDA complex in H_2O_2 treated leucocytes; H) Bright field image showing the actual cells; I) Dark field image showing reduced ROS level in LL12 treated cells; J) Bright field image showing the actual cells.

concentrations ($P > 0.05$).

3.9. Determination of intracellular ROS level in leucocytes

Gapeyev et al. [48] reported that H_2O_2 at concentrations $< 1\,\mu M$ did not induce any DNA damage to blood leukocytes in mice and at higher concentrations ($> 1\,\mu M$), DNA damage in cells was observed in a concentration dependant manner. It has been demonstrated that micromolar concentrations of H_2O_2 are able to activate systems of the antioxidant defense, including increasing the ROS scavenging activities of enzymes such as catalase, superoxide dismutase, glutathione reductase and glutathione peroxidase. Also, lower concentration of H_2O_2 stimulates the expression of the anti-apoptotic protein Bcl-2, thus protecting the cells from death. Thus the extracellular H_2O_2 has a major impact over the antioxidant mechanism of blood cells. In this regard, we employed FACS technique to analyse the DCF-fluorescence, a commonly used probe to assess the intracellular redox state and determined the changes in ROS level induced by LL12 on leucocytes at 2 h post-treatment with 30% of H_2O_2. Reduction in ROS level was observed at all tested doses of LL12 peptide (6.25, 12.5, 25, 50, 100, 200 μM); however, significant ($P < 0.05$) ROS scavenging effect were detected above 12.5 μM concentrations (Fig. 6A–F). Fluorescence micrographs of DCFH-DA stained cells that are treated with 12.5 μM of LL12 further confirmed the above fluorometric findings (Fig. 6G–J) where LL12-treated human blood leucocytes revealed a significantly lower level of DCF-fluorescence, compared with the control cells. Thus, it could be confirmed that LL12 peptide exhibit potential ROS scavenging activity and the LL12 peptide did not affect the total population of cells including monocytes, granulocyte and lymphocytes.

4. Conclusions

In conclusion, *A. platensis* is a potential cyanobacterium which can withstand the extreme level of oxidative stress induced by higher concentration of hydrogen peroxide and qRT-PCR analysis confirmed that the superoxide dismutase plays a key role in this antioxidant function. Additionally, this investigation highlights the free radical scavenging ability of the synthetic peptide, LL12 derived from the C-terminal SOD domain of *A. platensis*. Results indicated that the LL12 peptide has no cytotoxicity and potentially involved in reducing/scavenging the excess ROS produced in human leucocytes. Overall, the study suggested that *A. platensis* is an important source for the preparation of antioxidant peptides; and the oxidative stress reducing potency of LL12 peptide might have important applications in the healthcare, cosmetics and food industries.

Authors' contributions

Conceived and designed the experiments: AS, VK, MP, JA
Ethical clearance: MP
Performed the experiments: AS, VK, MP
Analysed the data: AS, VK, BA
Contributed reagents/materials/analysis tools: MKAS, JA
Wrote the paper: AS, VK, JA

Competing interests

The authors have declared that no competing interests exist.

Informed consent

For Blood collection, informed consent was obtained from all the participated adults in written form as per the protocol provided by CSIR-CDRI, Lucknow (Ethical Clearance No. CDRI/IEC/2014/A1).

Author agreement statement

The authors declare that this manuscript is original, has not been published before and is not currently being considered for publication elsewhere.

We confirm that the manuscript has been read and approved by all named authors and that there are no other persons who satisfied the criteria for authorship but are not listed. We further confirm that the order of authors listed in the manuscript has been approved by all of us. We understand that the Corresponding Author is the sole contact for the Editorial process. He is responsible for communicating with the other authors about progress, submissions of revisions and final approval of proofs.

Acknowledgement

References

[1] M. Valko, D. Leibfritz, J. Moncol, M.T.D. Cronin, M. Mazur, J. Telser, Free radicals and antioxidants in normal physiological functions and human disease, Int. J. Biochem. Cell Biol. 39 (2007) 44–84.

[2] L.S. Manley, Phytogenesis of halomethanes: a product of selection or a metabolic accident, Biogeochemistry 60 (2002) 163–180.

[3] W.J. Cooper, D.R.S. Lean, Hydrogen peroxide concentration in a northern lake: photochemical formation and die1 variability, Environ. Sci. Technol. 23 (1989) 1425–1428.

[4] H.H. Abd El-Baky, F.K. El Baz, G.S. El-Baroty, Enhancement of antioxidant production in *Spirulina platensis* under oxidative stress, Acta Physiol. Plant. 31 (2009) 623–631.

[5] T. Takeda, A. Yokota, S. Shigeoka, Resistance of photosynthesis to hydrogen peroxide in algae, Plant Cell Physiol. 36 (1995) 1089–1095.

[6] A. Caverzan, G. Passaia, S.B. Rosa, C.W. Ribeiro, F. Lazzarotto, M. Margis-Pinheiro, Plant responses to stresses: role of ascorbate peroxidase in the antioxidant protection, Genet. Mol. Biol. 35 (2012) 1011–1019.

[7] I. Fridovich, Superoxide radical and superoxide dismutases, Annu. Rev. Biochem. 64 (1995) 97–112.

[8] J. Wuerges, J.W. Lee, Y.I. Yim, H.S. Yim, S.O. Kang, K.D. Carugo, Crystal structure of nickel-containing superoxide dismutase reveals another type of active site, Proc. Natl. Acad. Sci. U. S. A. 101 (2004) 8569–8574.

[9] J. Arockiaraj, R. Palanisamy, P. Bhatt, V. Kumaresan, A.J. Gnanam, M. Pasupuleti, M. Kasi, A novel murrel Channa striatus mitochondrial manganese superoxide dismutase: gene silencing, SOD activity, superoxide anion production and expression, Fish Physiol. Biochem. 40 (2014) 1937–1955.

[10] V. Kumaresan, A.J. Gnanam, M. Pasupuleti, M.V. Arasu, N.A. Al-Dhabi, R. Harikrishnan, J. Arockiaraj, Comparative analysis of CsCu/ZnSOD defense role by molecular characterization: gene expression-enzyme activity-protein level, Gene 10 (2015) 53–62.

[11] M.M.S. Ismaiel, Y.M. El-Ayouty, P.C. Loewen, M.D. Piercey-Normore, Characterization of the iron-containing superoxide dismutase and its response to stress in cyanobacterium *Spirulina* (*Arthrospira*) *platensis*, J. Appl. Phycol. 26 (2014) 1649–1658.

[12] M.M. Abdel-Daim, S.M.M. Abuzead, S.M. Halawa, Protective role of *Spirulina platensis* against acute deltamethrin-induced toxicity in rats, PLoS One 8 (9) (2013).

[13] R. Konickova, K. Vankova, J. Vanikova, K. Vanova, L. Muchova, I. Subhanova, Anti-cancer effects of blue-green alga *Spirulina platensis*, a natural source of bilirubin-like tetrapyrrolic compounds, Ann. Hepatol. 13 (2014) 273–283.

[14] S. Ayehunie, A. Belay, T.W. Baba, R.M. Ruprecht, Inhibition of HIV-1 replication by an aqueous extract of *Spirulina platensis* (*Arthrospira platensis*), J. Acquir. Immune Defic. Syndr. Hum. Retrovirol. 18 (1998) 7–12.

[15] M.M. Abdel-Daim, S.M. Farouk, F.F. Madkour, S.S. Azab, Anti-inflammatory and immunomodulatory effects of *Spirulina platensis* in comparison to *Dunaliella salina* in acetic acid-induced rat experimental colitis, Immunopharmacol. Immunotoxicol. 37 (2015) 126–139.

[16] D. Remirez, R. González, N. Merino, S. Rodriguez, O. Ancheta, Inhibitory effects of *Spirulina* in zymosan-induced arthritis in mice, Mediat. Inflamm. 11 (2002) 75–79.

[17] C.M. Tayag, Y.C. Lin, C.C. Li, C.H. Liou, J.C. Chen, Administration of the hot-water extract of *Spirulina platensis* enhanced the immune response of white shrimp *Litopenaeusvannamei* and its resistance against *Vibrio alginolyticus*, Fish Shellfish Immun. 28 (2010) 764–773.

[18] P. Torres-Durán, R. Miranda-Zamora, M. Paredes-Carbajal, D. Mascher, J. Blé-Castillo, J. Dýaz-Zagoya, M. Juárez-Oropeza, Studies on the preventive effect of *Spirulina maxima* on fatty liver development induced by carbon tetrachloride, in the rat, J. Ethnopharmacol. 64 (1999) 141–147.

[19] M. Abdel-Daim, B.E. El-Bialy, H.G. Rahman, A.M. Radi, H.A. Hefny, A.M. Hassan,

Antagonistic effects of *Spirulina platensis* against sub-acute deltamethrin toxicity in mice: biochemical and histopathological studies, Biomed Pharmacother 77 (2016) 79–85.

[20] M. Khan, J.C. Shobha, I.K. Mohan, M.U.R. Naidu, C. Sundaram, S. Singh, et al., Protective effect of Spirulina against doxorubicin-induced cardiotoxicity, Phytother. Res. 19 (2005) 1030–1037.

[21] S.J. Lee, S.H. Cheong, Y.S. Kim, J.W. Hwang, H.J. Kwon, S.H. Kang, S.H. Moon, B.T. Jeon, B.J. Park, Antioxidant activity of a novel synthetic hexa-peptide derived from an enzymatic hydrolysate of duck skin by-products, Food Chem. Toxicol. 62 (2013) 276–280.

[22] X.R. Li, C.F. Chi, L. Li, B. Wang, Purification and identification of antioxidant peptides from protein hydrolysate of scalloped hammerhead (*Sphyrna lewini*) cartilage, Mar. Drugs 15 (2017) 61.

[23] Y. Wu, J. Wang, L. Li, X. Yang, J. Wang, X. Hu, Purification and identification of an antioxidant peptide from *Pinctada fucata* muscle, CyTA J. Food 16 (2018) 11–19.

[24] J. Yang, L. Hu, T. Cai, Q. Chen, Q. Ma, J. Yang, C. Meng, J. Hong, Purification and identification of two novel antioxidant peptides from perilla (*Perilla frutescens* L. Britton) seed protein hydrolysates, PLoS One (2018), https://doi.org/10.1371/journal.pone.0200021.

[25] Y. Jie, H. Yuanliang, X. Mingxiong, D. Yaohao, L. Shenao, P. Nan, L. Yunxiang, Z. Shumao, Purification and identification of antioxidant peptides from enzymatic hydrolysate of *Spirulina platensis*, J. Microbiol. Biotechnol. 26 (2016) 1216–1223.

[26] Y. Ren, H. Wu, X. Li, F. Lai, X. Xiao, Purification and characterization of high antioxidant peptides from duck egg white protein hydrolysates, Biochem. Biophys. Res. Commun. 452 (2014) 888–894.

[27] V. Kumaresan, F. Nizam, G. Ravichandran, K. Viswanathan, R. Palanisamy, P. Bhatt, M.V. Arasu, N.A. Al-Dhabi, K. Mala, J. Arockiaraj, Transcriptome changes of blue-green algae, *Arthrospira* sp. in response to sulfate stress, Algal Res. 23 (2017) 96–103.

[28] V. Kumaresan, A. Sannasimuthu, M.V. Arasu, N.A. Al-Dhabi, J. Arockiaraj, Molecular insight into the metabolic activities of a protein-rich micro alga, *Arthrospira platensis* by de novo transcriptome analysis, Mol. Biol. Rep. (2018), https://doi.org/10.1007/s11033-018-4229-1.

[29] H.K. Lichtenthaler, C. Buschmann, Chlorophylls and carotenoids: measurement and characterization by UV–VIS spectroscopy, Current Protocols in Food Analytical Chemistry (CPFA), John Wiley and Sons, New York, 2001, pp. F4.3.1–F4.3.8.

[30] C.F. Chi, B. Wang, Y.M. Wang, S.G. Deng, J.Y. Ma, Isolation and characterization of three antioxidant pentapeptides from protein hydrolysate of monkfish (*Lophius litulon*) muscle, Food Res. Int. 55 (2014) 222–228.

[31] W. Liao, Z. Ning, L. Ma, X. Yin, Q. Wei, E. Yuan, J. Yang, J. Ren, Recrystallization of dihydromyricetin from *Ampelopsis grossedentata* and its anti-oxidant activity evaluation, Rejuvenation Res. 17 (2014) 422–429.

[32] R. Re, N. Pellegrini, A. Proteggente, A. Pannala, M. Yang, C. Rice-Evans, Antioxidant activity applying an improved ABTS radical cation decolorization assay, Free Radic. Biol. Med. 26 (1999) 1231–1237.

[33] Y. Li, B. Jiang, T. Zhang, W. Mu, J. Liu, Antioxidant and free radical-scavenging activities of chickpea protein hydrolysate (CPH), Food Chem. 106 (2008) 444–450.

[34] C.P. Wan, E. Myung, B.H. Lau, An automated microfluorometric assay for monitoring oxidative burst activity of phagocytes, J. Immunol. Methods 159 (1993) 131–138.

[35] B. Demmig-Adams, W.I. Adams, Chlorophyll and carotenoid composition in leaves of *Euonymus kiautschovicus* acclimated to different degrees of light stress in the field, Funct. Plant Biol. 23 (1996) 649–659.

[36] M. Choudhary, U.K. Jetley, M. Abash Khan, S. Zutshi, T. Fatma, Effect of heavy metal stress on proline, malondialdehyde and superoxide dismutase activity in the cyanobacterium *Spirulina platensis*-S5, Ecotoxicol. Environ. Saf. 66 (2007) 204–209.

[37] K.H.S. Farvin, C.P. Baron, N.S. Nielsen, J. Otte, C. Jacobsen, Antioxidant activity of yoghurt peptides: part 2-characterisation of peptide fractions, Food Chem. 123 (2010) 1090–1097.

[38] K. Suetsuna, H. Ukeda, H. Ochi, Isolation and characterization of free radical scavenging activities peptides derived from casein, J. Nutr. Biochem. 11 (2000) 128–131.

[39] T.B. Zou, T.P. He, H.B. Li, H.W. Tang, E.Q. Xia, The structure–activity relationship of the antioxidant peptides from natural proteins, Molecules 21 (2016) 72.

[40] A. Davalos, M. Miguel, B. Bartolome, R. Lopez-Fandino, Antioxidant activity of peptides derived from egg white proteins by enzymatic hydrolysis, J. Food Protect. 67 (2004) 1939–1944.

[41] Elena Cojocaru, Nina Filip, Carmen Ungureanu, Cristiana Filip, Mihai Danciu, Effects of valine and leucine on some antioxidant enzymes in hypercholesterolemic rats, Health 6 (2014) 2313–2321.

[42] Z.J. Qian, W.K. Jung, H.G. Byun, S.K. Kim, Protective effect of an antioxidative peptide purified from gastrointestinal digests of oyster, *Crassostrea gigas* against free radical induced DNA damage, Bioresour. Technol. 99 (2008) 3365–3371.

[43] B. Wang, Z.R. Li, C.F. Chi, Q.H. Zhang, H.Y. Luo, Preparation and evaluation of antioxidant peptides from ethanol-soluble proteins hydrolysate of *Sphyrna lewini* muscle, Peptides 36 (2012) 240–250.

[44] H. Zhuang, N. Tang, Y. Yuan, Purification and identification of antioxidant peptides from corn gluten meal, J. Funct. Foods 5 (2013) 1810–1821.

[45] M.A. Cacciuttolo, L. Trinh, J.A. Lumpkin, G. Rao, Hyperoxia induces DNA damage in mammalian cells, Free Radic. Biol. Med. 14 (1993) 267–276.

[46] H. Guo, K. Yoshiaki, Y. Masami, Structures and properties of antioxidative peptides derived from royal jelly protein, Food Chem. 113 (2009) 238–245.

[47] Y.J. Gordon, E.G. Romanowski, A.M. McDermott, A review of antimicrobial peptides and their therapeutic potential as anti-infective drugs, Curr. Eye Res. 30 (2005) 505–515.

[48] A.B. Gapeyev, D.A. Yurshenas, A.A. Manokhin, The protection of DNA in blood leukocytes from damaging action of ultraviolet radiation using the "useful sun" strategy, Biophysics 62 (2017) 444–449.

[49] S. Cheng, M. Zhang, L. Sun, The iron-cofactored superoxide dismutase of Edwardsiella tarda inhibits macrophage-mediated innate immune response, Fish Shellfish Immunol. 29 (6) (2010) 972–978 (Dec).

[50] B.H. Kong, Y.L.L. Xiong, Antioxidant activity of zein hydrolysates in a liposome system and the possible mode of action, J. Agric. Food Chem. 54 (2006) 6059–6068.